

ASSESSMENT OF PERFORMANCE CHARACTERISTICS OF THE NICKEL-IRON CELL

V. S. MURALIDHARAN*, M. RAMAKRISHNAN, G. PARUTHIMAL KALAIANAN, K. GOPALAKRISHNAN and K. I. VASU

Central Electrochemical Research Institute, Karaikudi 623 006 (India)

(Received December 16, 1988; in revised form June 20, 1989)

Summary

Sintered iron and nickel electrodes were fabricated and 6 A h capacity cells were assembled. The performance characteristics of the individual electrodes and of the 6 A h cell have been assessed. For an ideal reversible battery, (dV/dQ) at a 50% state of discharge was used as the criterion for reversibility. Based on this, the role of iron and nickel electrodes in the assembled cells and the influence of temperature have been evaluated.

1. Introduction

The nickel-iron couple has been developed using cadmium-iron electrodes with mixtures of iron, cobalt, nickel oxides, and FeS as base materials since 1901. Cylindrical positive tubes, copper-iron electrodes, and non-tubular electrodes have all been used in nickel-iron cells [1 - 4]. Porous, sintered substrates are being developed to increase the efficiency of the active material with higher surface area powders and pore sizes below 20 μm . A nickel foam structure with a porosity of 85% or more has been achieved [5] without any decrease in mechanical strength. Interest in using the iron electrode has increased because of its high theoretical specific capacity, low cost per ampere hour, the abundance of iron in nature, and its non-toxicity.

2. Experimental

Preparation of sintered negative electrodes

Table 1 gives the properties of the powders used to prepare the electrodes. Electrolytic iron powder was reduced at 870 K for 2 h under a hydrogen atmosphere. Loose, sintered iron electrodes were prepared from

* Author to whom correspondence should be addressed.

TABLE 1
Chemical and physical properties of powders used

Powder	Chemical composition (%)	Apparent density (g cm^{-3})	Tap density (g cm^{-3})	Particle size (μm)	Specific surface area* ($\text{m}^2 \text{g}^{-1}$)
Electrolytic iron	99 Fe; 0.0001 Pb; 0.008 Zn; 0.001 As; 0.025 Mn; 0.005 Cu	2.84	3.08	≤ 37	11.08
Synthetic black iron oxide (Fe_3O_4)	96.99 Fe_3O_4 ($\text{Fe}^{2+} = 44.55$; $\text{Fe}^{3+} = 25.73$)	1.22	1.71	≤ 37	38.72
Electrolytic copper	99.5 Cu	—	—	≤ 37	14.21
Cadmium oxide (CdO)	99.5 (Ex, Cd); 0.0015 Fe; 0.005 K; 0.01 Na	—	—	≤ 37	11.89
INCO nickel 255	$< 0.20 \text{ C}$ $< 0.15 \text{ O}$, $< 0.001 \text{ S}$, $< 0.01 \text{ Fe}$ Remaining nickel	0.5 - 0.65	—	2.2 - 3.0	—

* BET method (Quantasorb using liquid nitrogen).

iron powder mixed with 15 wt.% iron oxide, 3 wt.% copper and 0.3 wt.% ferrous sulphide powder. This powder was spread uniformly over a 0.2 mm thick perforated, nickel-plated, mild steel grid. The $7 \times 5.5 \times 0.2$ cm electrodes were sintered at 1173 K for 1 h under hydrogen. The electrodes were cathodically treated in 6.0 M KOH solution containing 32 g l^{-1} of elemental sulphur using a stainless steel anode [6]. The porosities of the electrodes, employing the xylene impregnation method [7], were from 55 to 65%.

Preparation of sintered positive electrodes

Chemical impregnation

Porous nickel electrodes were prepared from previously reduced INCO nickel 255 powder. Nickel plaques were prepared with the same sized grid as that of the iron electrode and sintered, under hydrogen, at 1173 K for 45 min. The porosities were between 75 and 80%. Active material was vacuum impregnated into the sintered electrode from a nickel nitrate bath [8]. It was then cathodically treated in an alkaline solution using a nickel anode and finally washed free from nitrate ions. This sequence of operations was repeated 6 - 8 times until there was no weight gain.

Electrochemical impregnation

The preparation procedure for loose, sintered electrodes was the same as that for chemically impregnated electrodes. They were impregnated cathodically in a solution prepared from 3 M $\text{Ni}(\text{NO}_3)_2$ with additives such as 0.3 M Co^{2+} , 0.1 M Cd^{2+} , 0.1 M Mn^{2+} , and 0.1 M Zn^{2+} salts (pH 2 - 3) using nickel anodes. The electrodes were dried and dipped in a 6 M KOH solution at 353 K for 1 h. The electrodes were washed free from nitrate ion, held in double-distilled water for 30 min, and finally dried. The impregnation sequence was repeated until a constant gain in weight was observed.

Charge-discharge of the nickel electrode

Miniature cells were assembled with a single nickel electrode and two, higher capacity, iron counter electrodes. The electrolyte was 6 M KOH containing 0.63 M LiOH, and the separator was nylon cloth. The capacity of the chemically impregnated nickel electrode was 1.2 - 1.6 A h at a 6 h discharge rate, whilst that of the electrochemically impregnated nickel electrode was 1.8 - 2.0 A h at the same rate. The cell was charged at a C/13 rate for 20 h at constant current. Discharge studies were carried out at C/10, C/6, C/4, and C/3 rates using a manually adjusted rheostat to maintain constant current. The potential of the nickel electrode *versus* an Hg/HgO reference electrode was recorded at 303 K. Different depths of discharge were made at the C/4 rate for the chemically impregnated nickel electrodes.

Charge-discharge of the iron electrode

A miniature cell was assembled with a single iron electrode and two higher capacity nickel counter electrodes using the same electrolyte and separator as above. The capacity of the iron electrode was 1.8 - 2.0 A h at the 6 h discharge rate. The cell was charged at the $C/13$ rate in constant current mode and discharge studies were carried out at $C/6$, $C/4$, and $C/3$ rates using a rheostat. The potential of the iron electrode *versus* an Hg/HgO reference electrode and the cell voltage was measured as above, but in this case the $C/6$ rate was used for the depth of discharge studies.

Charge-discharge characteristics of assembled 6 A h cells

Two types of cells were assembled:

(a) with four chemically impregnated nickel electrodes and three iron electrodes;

(b) with four electrochemically impregnated nickel electrodes and five iron electrodes.

Each was placed in a perspex container with a nylon cloth separator and 6.0 M KOH + 0.63 M LiOH electrolyte. The capacity of both types of cell was 6 A h at the $C/6$ discharge rate at 303 K. They were charged at the $C/15$ rate in constant current mode. Discharge studies were carried out at rates of $C/6$, $C/4$, and $C/3$. Different depths of discharge were made at the $C/6$ rate for the chemically impregnated nickel electrode cell.

3. Results and discussion

In the potential *versus* delivered capacity curves at different discharge rates for a nickel electrode (Fig. 1), the initial fall from 500 mV to 350 mV is due to the activation over-potential losses; an almost linear voltage loss

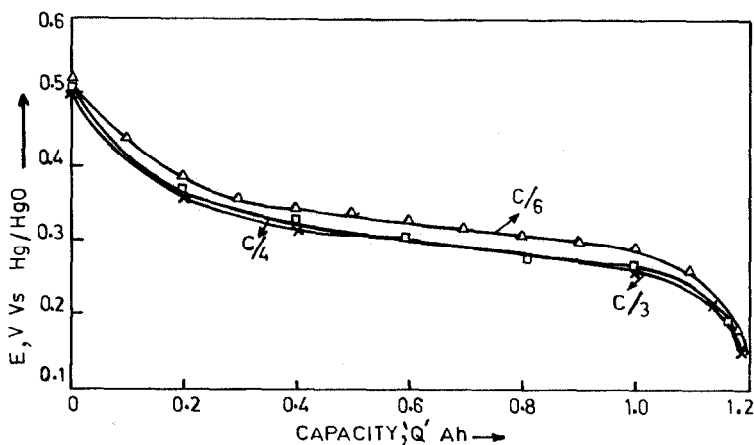


Fig. 1. Electrode potential *vs.* capacity curves for chemically-impregnated nickel electrode during discharge at different rates.

between 0.3 and 1.0 A h is virtually wholly due to the internal resistance and polarisation resistance components of the electrode reaction, and the final voltage fall-off is due to the diffusion of hydroxyl ions into the pores. On repeated cycling (Fig. 2) the slope of the initial voltage loss increases, while the length of the "Constant-potential" plateau decreases because of the formation of $\text{Ni}_3\text{O}_2(\text{OH})_4$ [8].

In the case of the electrochemically impregnated nickel electrode (Fig. 3) the initial fall from 440 mV to 300 mV occurs within 15% of the capacity being used. It is due to the activation over-potential losses. The "plateau" (280 - 240 mV) extends from 15% to 90% of the total capacity: mass transport effects limit performance beyond this.

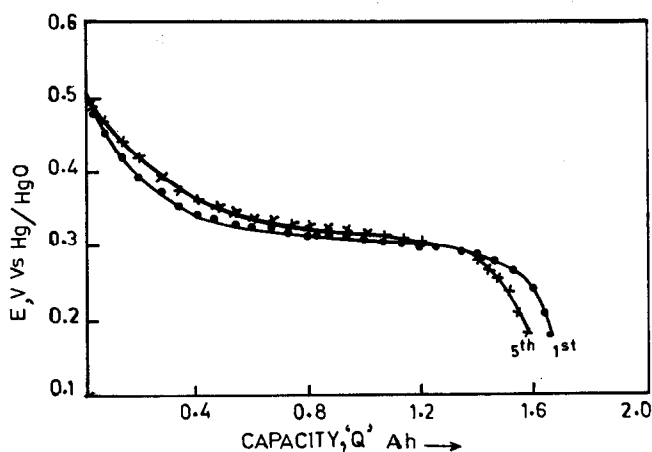


Fig. 2. Electrode potential vs. capacity curves for chemically-impregnated nickel electrode during discharge at $C/4$ rate — effect of cycling.

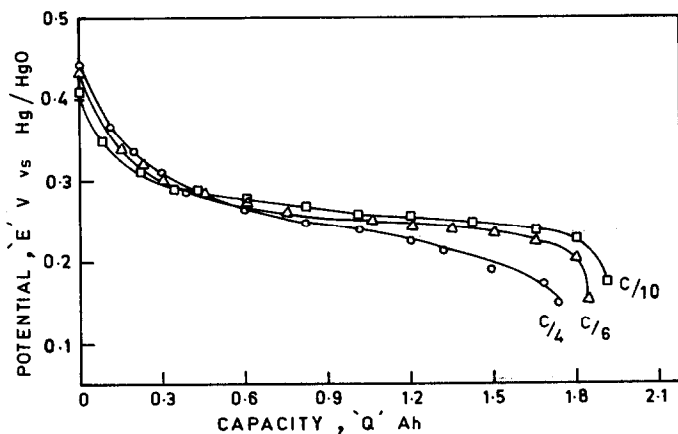


Fig. 3. Electrode potential vs. capacity curves for electrochemically-impregnated nickel electrode during discharge at different rates.

Studies of variation in the electrode potential *versus* capacity for the iron electrode at different discharge rates (Fig. 4) showed that there is a rapid initial decrease in the potential from -975 mV to -875 mV. This is essentially because of oxidation of the adsorbed hydrogen and partial oxidation of the surface. The appearance of the plateau at -875 mV is due to the oxidation [9, 10] of iron to $\text{Fe}(\text{OH})_2$ and of $\text{Fe}(\text{OH})_2$ to FeOOH . This region accounts for between 12% and 85% of the capacity.

The limiting region from -875 mV to -800 mV is due to the diffusion of hydroxyl ions inside the pores and other mass transport limitations. Figure 5 shows that 90% of the entire capacity is delivered at about -875 mV, perhaps because more and more active sites are exposed to the electrolyte. At the same time, after 5 cycles, the potential is seen to be sustained for longer periods suggesting the conversion of Fe to $\text{Fe}(\text{OH})_2$ rather than further oxidation of $\text{Fe}(\text{OH})_2$. Better reversibility is obtained when the number of cycles is increased.

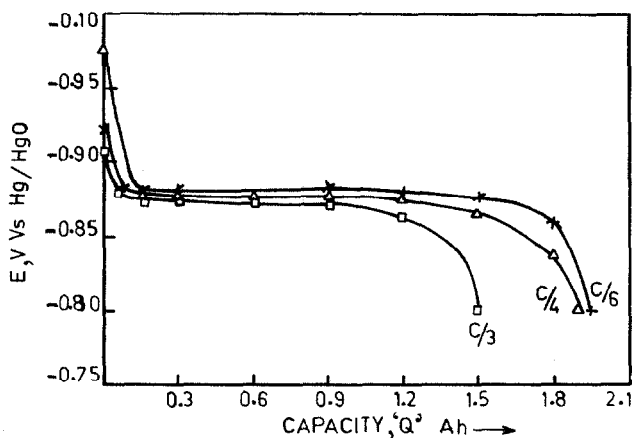


Fig. 4. Electrode potential *vs.* capacity curves for iron electrode during discharge at different rates.

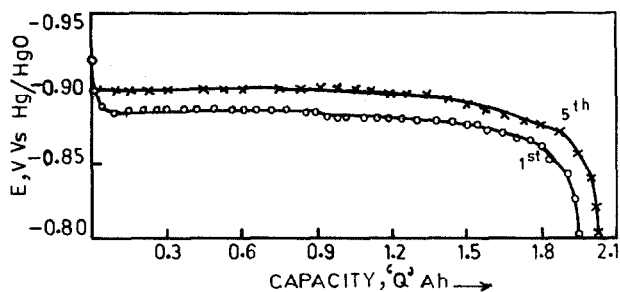


Fig. 5. Electrode potential *vs.* capacity curves for iron electrode during discharge at $C/6$ rate during the 1st and 5th cycles.

The discharge characteristics of the 6 A h cell, consisting of four chemically impregnated nickel and three iron electrodes, at 303 K and different discharge rates are shown in Fig. 6. The cell voltage falls about 200 mV during delivery of the first 30% of the capacity. The change in voltage is then much reduced until about 75% of the capacity is used at which point it starts to fall again, even at the $C/3$ discharge rate. The characteristics at the $C/6$ rate of discharge of the first, fifth, and eighth cycles

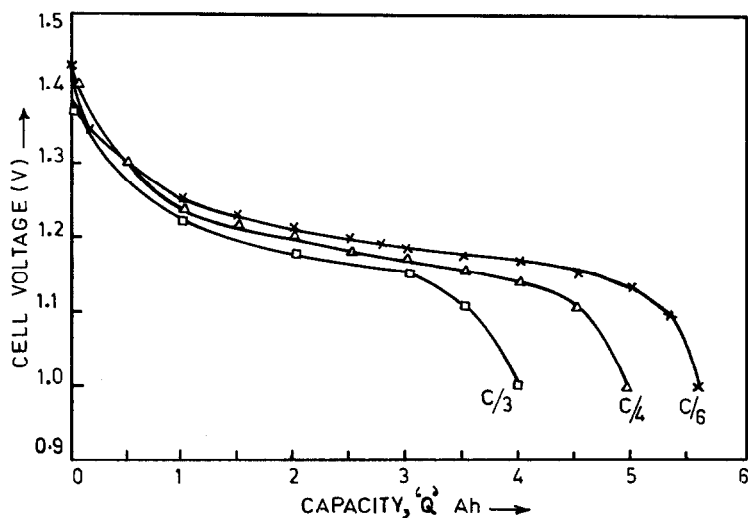


Fig. 6. Cell voltage vs. capacity curves for chemically-impregnated nickel/iron cell at different discharge rates.

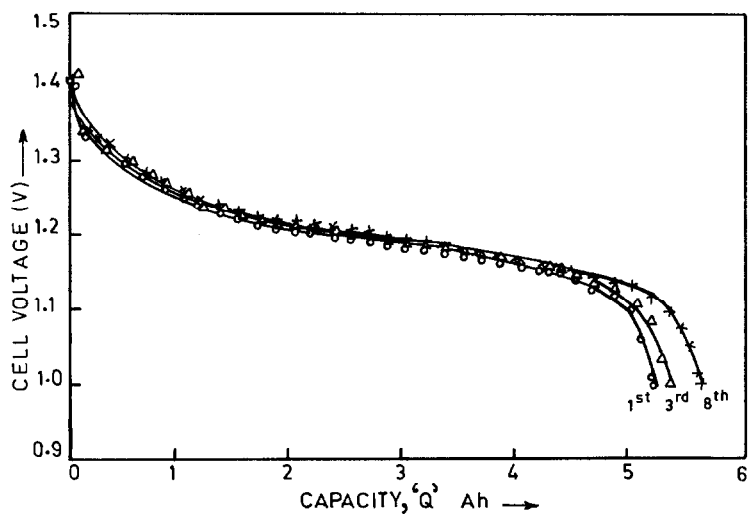


Fig. 7. Cell voltage vs. capacity curves for chemically-impregnated nickel/iron cell during discharge at $C/6$ rate during the 1st, 3rd, and 8th cycles.

are shown in Fig. 7. The only significant change is the increase in capacity with cycle number.

A 6 A h cell, consisting of four electrochemically impregnated nickel and five iron electrodes, was charged at the $C/15$ rate. The discharge characteristics of the cell at 303 K and different discharge rates are shown in Fig. 8. They are similar to those of the chemically impregnated electrodes except that the initial voltage losses are lower, while the onset of the voltage decay at the end of life is not as sudden, extending to 83% of the capacity even at the $C/2$ rate.

Figure 9 shows the influence of temperature on the discharge characteristics of this 6 A h cell which exhibits a loss of both voltage and capacity as the temperature falls from 323 K to 283 K. This may be due to enhanced hydroxyl ion transport within the electrode pores.

An ideal reversible battery requires that the slope of the open-circuit-voltage *versus* the state-of-discharge curve (V *versus* Q) be zero in the absence of activation over-potential, diffusion over-potential, internal resistance and other complications arising out of design. Since a near constant voltage in the discharge curves was obtained between 12% and 86% utilization for single electrodes and assembled cells (dV/dQ) a 50% state of discharge was used to compare the reversible behaviour of the assembled cell and electrodes [11]. Table 2 presents the parameters derived from the discharge curves at different rates. The (dV/dQ) values are less for the iron electrodes than for both types of nickel electrode. Of the nickel electrodes, the slope using those which were chemically impregnated was greater than when they were electrochemically impregnated. It appears that the overall cell behaviour is controlled by the performance of the nickel electrodes.

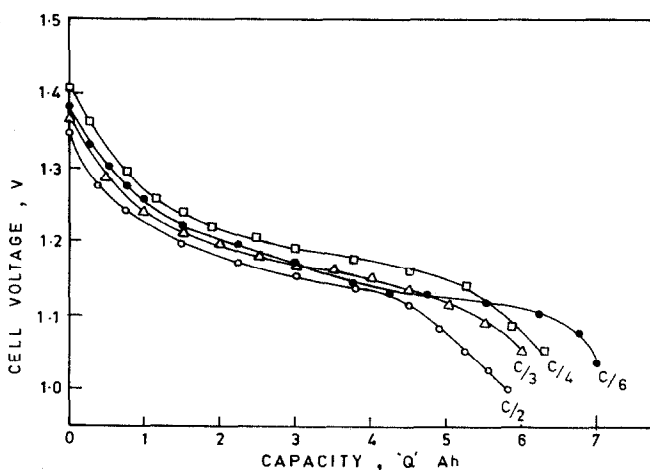


Fig. 8. Cell voltage *vs.* capacity curves for electrochemically-impregnated nickel/iron cell during discharge at different rates.

TABLE 2

Parameters derived from discharge curves at different rates

Discharge rate	Iron electrode ($dE^-/dQ) \times 10^{-3}$ (V C $^{-1}$) ($Q = Q_0^-/2$)	Nickel electrode ($dE^+/dQ) \times 10^{-3}$ (V C $^{-1}$) ($Q = Q_0^+/2$)		Cell ($dV/dQ) \times 10^{-3}$ (V C $^{-1}$) ($Q = Q_0/2$)
		Chemically impregnated	Electrochemically impregnated	
C/10	—	—	33.3	—
C/6	8.33	70.0	16.5	20
C/4	8.33	87.5	33.3	25
C/3	12.50	87.5	—	30
C/2	—	—	—	20

C = Capacity of the assembled cell (6 A h), discharge is carried out till 1.0 V is reached. Capacity of the iron electrode (1.8 A h), discharge is carried out till -0.8 V vs. Hg/HgO is reached.

Capacity of the chemically impregnated nickel electrode (1.2 A h) and for electrochemically impregnated (2.0 A h) discharge is carried out till 0.2 V vs. Hg/HgO is reached.

V C $^{-1}$ = Volts Coulomb $^{-1}$.

TABLE 3

Parameters derived from discharge curves — effect of cycling

No. of cycles	Iron electrode ($dE^-/dQ) \times 10^{-3}$ (V C $^{-1}$) ($Q = Q_0^-/2$)	Chemically impregnated nickel electrode ($dE^+/dQ) \times 10^{-3}$ (V C $^{-1}$) ($Q = Q_0^+/2$)	Chemically impregnated nickel electrode cell ($dV/dQ) \times 10^{-3}$ (V C $^{-1}$) ($Q = Q_0/2$)
1	8.33	70.0	17.0
2	8.33	25.0	20.0
3	4.17	25.0	22.5
4	4.17	25.0	22.5

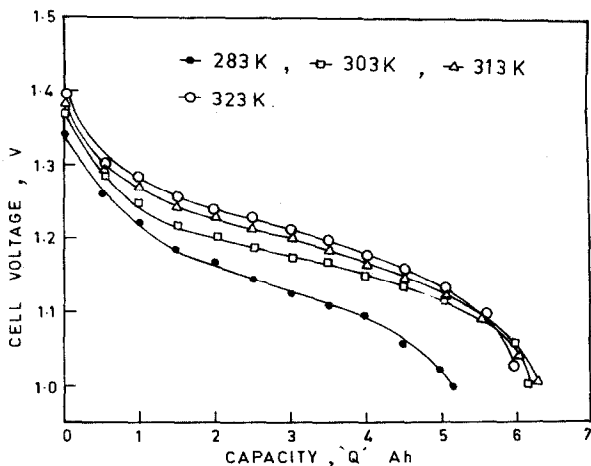


Fig. 9. Cell voltage vs. capacity curves for electrochemically-impregnated nickel/iron cell during discharge at $C/3$ rate at different temperatures.

On repeated cycling at the $C/6$ rate, the value of the slope decreases for the iron electrode and increases for the chemically impregnated nickel electrode (Table 3). Although the iron electrodes appear to be more reversible, the performance of the cell on repeated cycling is controlled by other factors, such as oxygen and hydrogen evolution reactions. Table 4 shows the influence temperature has on the parameters derived from cell performance curves using electrochemically impregnated nickel electrodes. The (dV/dQ) value is at a minimum at 303 K while moderate at 313 K and 323 K.

TABLE 4

Parameters derived from discharge curves at $C/3$ rate — influence of temperature

Temperature (K)	Electrochemically impregnated nickel electrode cell $(dV/dQ) \times 10^{-3} (V C^{-1})$ ($Q = Q_0/2$)
283	45
303	20
313	30
323	30

4. Conclusions

Sintered iron- and nickel-electrodes were fabricated and 6 A h cells were assembled. An analysis of the discharge curves revealed that the

performance of the cell is closer to that of the nickel electrode than to that of the iron electrode. On repeated charge-discharge cycling, the performance of the assembled chemically impregnated nickel electrode is assumed to be controlled by oxygen and hydrogen evolution reactions. The assembled cell using electrochemically impregnated nickel electrodes performs well above 303 K and moderate performance was observed between 313 K and 323 K.

References

- 1 Westinghouse Electric Corporation, Final Report — Design and cost study of a nickel/iron oxide battery for electric vehicles, Volume II: Public Report, *ERDA Rep. No. ANL-K-77-3723-1*. August 1977.
- 2 S. U. Falk and A. J. Salkind, *Alkaline Storage Batteries*, Wiley, New York, 1969.
- 3 Eagle-Pitcher Industries Inc., Annual Report for 1978 on research, development and demonstration of nickel/iron batteries for electric vehicle propulsion, *Argonne Nat. Lab. Rep., ANL/OEPM-78-13*, October 1979.
- 4 SAFT Storage Battery Division, *SAFT sintered plate sealed cells, VR VB Vx*, 1974, pp. 3 - 11.
- 5 T. Iwaki, N. Yanagihara and H. Ogawa, *Prog. Batteries Sol. Cells*, 4 (1982) 125.
- 6 R. J. McCornmick, Yorktown Heights, and W. E. Ryan, Pleasant Ville, NY, U.S. *Pat. 3 525.640* (1970).
- 7 L. Ojefers, *J. Electrochem. Soc.*, 123 (1976) 1139.
- 8 G. Paruthimal Kalaignan, V. S. Muralidharan and K. I. Vasu, *Proc. 10th Int. Congr. Metallic Corrosion, Madras, India, Nov. 7 - 11, 1987*, Vol. 1, Oxford and IBH Publishing, 1987, p. 615.
- 9 G. Paruthimal Kalaignan, V. S. Muralidharan and K. I. Vasu, *J. Appl. Electrochem.*, 17 (1987) 1083.
- 10 G. Paruthimal Kalaignan, V. S. Muralidharan and K. I. Vasu, *Trans. Soc. Adv. Electrochem. Sci. Technol.*, 22 (1987) 67.
- 11 S. Satyanarayana, *Trans. Soc. Adv. Electrochem. Sci. Technol.*, 11 (1976) 19.